Published as: *Nature*. 2009 March 19; 458(7236): 351–356.

Regulatory T-cell suppressor program co-opts transcription factor IRF4 to control T_H2 responses

Ye Zheng[1,2,†], **Ashutosh Chaudhry**[1,2,†], **Arnold Kas**[1,2], **Paul deRoos**[1,2,†], **Jeong M. Kim**[1,2], **Tin-Tin Chu**[1,2], **Lynn Corcoran**[4], **Piper Treuting**[3], **Ulf Klein**[5], and **Alexander Y. Rudensky**[1,2,†]

[1]Howard Hughes Medical Institute, University of Washington, Seattle, Washington 98195, USA

[2]Department of Immunology, University of Washington, Seattle, Washington 98195, USA

[3]Department of Comparative Medicine, University of Washington, Seattle, Washington 98195, USA

[4]Immunology Division, The Walter and Eliza Hall Institute, Parkville Victoria 3050, Australia

[5]Institute for Cancer Genetics and Herbert Irving Comprehensive Cancer Center, Columbia University, New York, New York 10032, USA

Abstract

In the course of infection or autoimmunity, particular transcription factors orchestrate the differentiation of T_H1, T_H2 or T_H17 effector cells, the responses of which are limited by a distinct lineage of suppressive regulatory T cells (T_{reg}). T_{reg} cell differentiation and function are guided by the transcription factor Foxp3, and their deficiency due to mutations in Foxp3 results in aggressive fatal autoimmune disease associated with sharply augmented T_H1 and T_H2 cytokine production[1–3]. Recent studies suggested that Foxp3 regulates the bulk of the Foxp3-dependent transcriptional program indirectly through a set of transcriptional regulators serving as direct Foxp3 targets[4,5]. Here we show that in mouse T_{reg} cells, high amounts of interferon regulatory factor-4 (IRF4), a transcription factor essential for T_H2 effector cell differentiation, is dependent on Foxp3 expression. We proposed that IRF4 expression endows T_{reg} cells with the ability to suppress T_H2 responses. Indeed, ablation of a conditional *Irf4* allele in T_{reg} cells resulted in selective dysregulation of T_H2 responses, IL4-dependent immunoglobulin isotype production, and tissue lesions with pronounced plasma cell infiltration, in contrast to the mononuclear-cell-dominated pathology typical of mice lacking T_{reg} cells. Our results indicate that T_{reg} cells use components of the transcriptional machinery, promoting a particular type of effector $CD4^+$ T cell differentiation, to efficiently restrain the corresponding type of the immune response.

T_{reg} cell deficiency results in activation and expansion of $CD4^+$ and $CD8^+$ T cells, dendritic cells, granulocytes and macrophages, and greatly increased production of a wide range of cytokines including interleukin (IL)-2, T_H1 and T_H2 cytokines[6,7]. Expression of Foxp3 is required for the establishment and maintenance of T_{reg} lineage identity and suppressor function[8–11]. Our recent study suggested that in T_{reg} cells Foxp3 might regulate expression of IRF4 (refs 12–14) a transcription factor that is indispensable for T_H2 effector cell differentiation[15,16]. Furthermore, a recent study suggested a prominent role for IRF4 in T_H17

Correspondence and requests for materials should be addressed to A.Y.R. (rudenska@mskcc.org).
[†]Present address: Department of Immunology, Memorial Sloan-Kettering Cancer Center, New York, New York 10021, USA.

Supplementary Information is linked to the online version of the paper at www.nature.com/nature.

Author Information Reprints and permissions information is available at www.nature.com/reprints.

Full Methods and any associated references are available in the online version of the paper at www.nature.com/nature.

differentiation[17]. Thus, we decided to examine a role for IRF4 in T_{reg} cell differentiation and function.

Foxp3 binding within the promoter region of *Irf4* in T_{reg} cells[4] was confirmed by chromatin immunoprecipitation (ChIP)-coupled quantitative PCR (qPCR) (Supplementary Fig. 1a, b). *Irf4* messenger RNA was increased in thymic and peripheral Foxp3$^+$ T_{reg} cells in comparison to CD25$^-$ Foxp3$^-$ CD4$^+$ T cells (data not shown)[8]. Furthermore, Foxp3 knockdown using a retrovirally encoded Foxp3-specific short hairpin RNA resulted in a marked diminution in *Irf4* mRNA (Supplementary Fig. 1c), suggesting that Foxp3 directly regulates IRF4 expression in T_{reg} cells.

Next we induced deletion of a conditional *Irf4* allele (*Irf4^{fl}*) in T_{reg} cells by crossing *Irf4^{fl}* mice to *Foxp3^{Cre}* mice expressing yellow fluorescent protein (YFP)-Cre recombinase fusion protein under the *Foxp3* locus control[18,19]. The *Irf4^{fl}* allele has a 'built-in' reporter capacity in that Cre-mediated recombination results in the deletion of the *Irf4* promoter and the exon containing the translational start, and the concomitant expression of green fluorescent protein (GFP)[18]. The specificity of the *Irf4^{fl}* deletion was examined by flow cytometric analysis of Foxp3 expression in a sorted GFP$^+$ CD4$^+$ T cell population that underwent Cre-mediated recombination, and in a GFP$^-$ CD4$^+$ T cell population that did not. Essentially all GFP$^+$ cells expressed Foxp3, whereas GFP$^-$ cells lacked Foxp3 expression (Fig. 1a). Flow-cytometric analysis of control *Irf4$^{fl/+}$ Foxp3^{Cre}* mice showed that IRF4 expression was markedly increased in all peripheral T_{reg} cells, but only modestly in Foxp3$^+$ CD4$^+$ thymocytes, whereas IRF4 levels were undetectable in corresponding Foxp3$^-$ cell subsets. On Cre-mediated deletion in *Irf4$^{fl/fl}$Foxp3^{Cre}* mice, IRF4 protein became undetectable in both peripheral and thymic Foxp3$^+$ cells (Fig. 1b). *Irf4$^{fl/fl}$Foxp3^{Cre}* and *Irf4$^{fl/-}$ Foxp3^{Cre}* mice harbouring an IRF4-deficient T_{reg} subset were born at the expected Mendelian ratio and were indistinguishable from their wild-type or heterozygous littermates during the first month of life. However, by 6–8 weeks of age *Irf4$^{fl/fl}$Foxp3^{Cre}* and *Irf4$^{fl/-}$ Foxp3^{Cre}* mice manifested identical autoimmune disease—including lymphadenopathy, weight loss, blepharitis and dermatitis—and succumbed to disease at 3–4 months of age (Fig. 1c, d and data not shown). Histopathological evaluation of diseased mice showed massive infiltration in the pancreas, lung and stomach, whereas control littermates did not show any noticeable pathology. For comparison to a complete T_{reg} cell deficiency, we analysed tissue lesions in *Foxp3^{DTR}* knock-in mice (expressing human diphtheria receptor, DTR under control of *Foxp3* locus) that were subjected to chronic ablation of a T_{reg} cell subset caused by diphtheria toxin treatment, starting from birth. These mice showed analogous lesions in the pancreas and stomach, and much more severe lesions in the lung in comparison to mice harbouring an IRF4-deficient T_{reg} subset (Fig. 1e and data not shown). In contrast to the massive liver lesions observed after T_{reg} depletion, livers in mice containing an IRF4-deficient T_{reg} subset were unaffected, but kidneys showed the opposite trend (Supplementary Fig. 2 and data not shown). Furthermore, flow cytometric analysis showed expansion and activation of peripheral T cells but not dendritic cells in *Irf4$^{fl/fl}$Foxp3^{Cre}* mice, in contrast to the increased numbers of activated dendritic cells observed in T_{reg}-deficient mice (Fig. 2a, b and data not shown).

The aforementioned phenotypic differences between mice lacking T_{reg} cells and mice containing IRF4-deficient T_{reg} cells could be due to a numerical decrease in the T_{reg} cells in the absence of IRF4. However, the IRF4-deficient T_{reg} subset was markedly increased in diseased *Irf4$^{fl/fl}$Foxp3^{Cre}* mice compared to *Irf4$^{fl/+}$ Foxp3^{Cre}* littermate controls, probably in response to T cell activation (Fig. 2c, d). IRF4 deficiency did not change Foxp3 protein expression on a per cell basis (Fig. 2c), excluding the possibility of down-modulation of Foxp3 in T_{reg} cells in the absence of IRF4 as a reason for their functional incompetence. These results pointed to impairment in a particular aspect of T_{reg} function on IRF4 ablation.

Indeed, analysis of cytokine production by CD4$^+$ T cells from *Irf4$^{fl/fl}$Foxp3^{Cre}* mice showed a notable increase in the numbers of IRF4-sufficient Foxp3$^-$ CD4$^+$ T cells producing the T_H2 cytokines IL-4 and IL-5 (Fig. 3a, b), whereas IRF4-deficient Foxp3$^+$ T_{reg} cells, unlike their IRF4-sufficient counterparts, were unable to produce effector cytokines (Supplementary Fig. 3). The production of IL-2 and the T_H1 cytokine IFN-γ by CD4$^+$ T cells was largely unchanged, but production of the T_H17 cytokine IL-17 was marginally increased in *Irf4$^{fl/fl}$Foxp3^{Cre}* mice compared to *Irf4$^{fl/+}$ Foxp3^{Cre}* controls (Fig. 3a, b and data not shown). In agreement with these results, enzyme-linked immunosorbent assay (ELISA) showed high amounts of the T_H2 cytokines IL-5, IL-13 and IL-10 in the supernatants of CD3-stimulated splenic *Irf4$^{fl/fl}$Foxp3^{Cre}* T cell cultures (Supplementary Fig. 4). In contrast, a lack of T_{reg} cells in *Foxp3$^-$* mice led to sharply increased production of IFN-γ and IL-4 by CD4$^+$ T cells (Supplementary Fig. 5). Massive increases in IFN-γ and IL-2 production were also observed after ablation of T_{reg} cells in *Foxp3^{DTR}* mice[7] (J. M. Lund and A.Y.R., unpublished observations). Thus, T_H2 effector CD4$^+$ T cell responses seem to be selectively dysregulated in mice containing IRF4-deficient T_{reg} cells. Notably, the augmented T_H2 responses appeared in *Irf4$^{fl/fl}$Foxp3^{Cre}* mice only by 3–4 weeks of age, whereas both T_H2 and T_H1 cytokine production in 11-day-old *Irf4$^{fl/fl}$Foxp3^{Cre}* and *Irf4$^{fl/+}$ Foxp3^{Cre}* mice was low (data not shown).

Because IL-4 is an important cytokine that promotes IgG1 and IgE class-switch recombination, we measured levels of serum immunoglobulin isotypes in diseased 8-week-old *Irf4$^{fl/fl}$Foxp3^{Cre}* and littermate control *Irf4$^{fl/+}$ Foxp3^{Cre}* mice. As a positive control, we also analysed 3–4-week-old T_{reg}-deficient *Foxp3$^-$* mice. Consistent with an uncontrolled T_H2 response, IL-4-dependent IgG1 and IgE serum concentrations reached very high levels (10–30 mg ml^{-1} and 0.75–1.5 mg ml^{-1}, respectively) in *Irf4$^{fl/fl}$Foxp3^{Cre}* mice, whereas serum IgM and IgA concentrations were only modestly increased in comparison to control mice. However, the amounts of the remaining immunoglobulin isotypes, including IFN-γ-dependent IgG2a, were diminished in the serum of afflicted mice (Fig. 4a). Unlike *Irf4$^{fl/fl}$Foxp3^{Cre}* mice, *Foxp3$^-$* mice showed in addition to increased IgG1 and IgE, sharply increased amounts of IgG2a consistent with the increased IFN-γ production in these mice (Fig. 4a). Furthermore, we observed ubiquitous germinal centre formation and increased numbers of plasma cells in the spleens of diseased *Irf4$^{fl/fl}$Foxp3^{Cre}* mice, but not in the littermate controls (Fig. 4b and data not shown). In *Irf4$^{fl/fl}$Foxp3^{Cre}* mice, 15% and 67% of plasma cells produced IgE and IgG1, respectively, in contrast to 3% IgG1-producing and undetectable numbers of IgE-producing plasma cells in control mice (Supplementary Fig. 6). Furthermore, examination of diseased mice harbouring an IRF4-deficient T_{reg} cell subset revealed a predominance of cells with a characteristic plasma cell morphology infiltrating the pancreas, kidney and stomach (Fig. 4c and data not shown). In contrast, the pancreatic and other tissue infiltrates in *Foxp3^{DTR}* mice subjected to chronic T_{reg} ablation, or in *Foxp3$^-$* mice, consisted predominantly of macrophages, lymphocytes and neutrophils with very few plasma cells (Fig. 4c and data not shown). We also tested whether the dysregulated T_H2 response in the presence of IRF4-deficient T_{reg} cells promoted autoantibody production. Indeed, serum IgG1 from affected *Irf4$^{fl/fl}$Foxp3^{Cre}* mice showed robust reactivity with several tissue antigens, whereas minimal reactivity was found in control animals (Supplementary Fig. 7).

The distinct immune activation profile and tissue lesions in diseased mice harbouring an IRF4-deficient T_{reg} cell subset were in agreement with the previously mentioned idea that only a part of the suppressor program was impaired in IRF4-deficient T_{reg} cells. In further support of this notion, the *in vitro* suppressor capacity of IRF4-deficient T_{reg} cells isolated from *Irf4$^{fl/fl}$Foxp3Cre* mice was largely intact (Fig. 5a). Furthermore, cell surface amounts of two putative T_{reg} suppressor effector molecules CTLA4 and CD73 (also known as NT5E) were not altered in IRF4-deficient T_{reg} cells. The levels of CD25 (IL2RA) and GITR (TNFRSF18) were also unchanged (Fig. 5b and data not shown). However, ICOS expression was decreased,

suggesting that IRF4 regulates expression of a distinct subset of functionally important genes in T_{reg} cells.

An unbiased assessment of the effect of IRF4 deficiency on T_{reg} transcriptome demonstrated that the expression of up to 20% of 'T_{reg}-specific' genes decreased in the absence of IRF4, whereas approximately 7% were increased (Fig. 5c). Recent gene targeting studies demonstrated that T_{reg} cells use several suppressor modalities[19–25]. Examination of the IRF4-dependent subset of 'T_{reg}' genes and the subsequent independent confirmation by qPCR showed significantly decreased expression of several genes (*Fgl2*, *Il10* and *Gzmb*) encoding putative suppressor effector molecules; a few (*Ebi3* and *Entpd1*) were only marginally decreased, whereas others (*Tgfb1* and *Ctla4*) did not change (Fig. 5d, e and data not shown). It is likely that changes in expression of a combination of genes, but not a single gene, account for the impaired suppressor capacity of IRF4-deficient T_{reg} cells. In this regard, we recently showed a role for IL10 in T_{reg}-mediated suppression[20]. In addition, ICOS-deficient T_{reg} cells were inferior in comparison to their wild-type counterparts in limiting expansion of effector T cells in lymphopenic hosts (Y.Z., unpublished observations).

The observation that ICOS—the expression of which is critically important for T_H2 differentiation[26]—was expressed in T_{reg} cells in an IRF4-dependent manner suggested that IRF4 might be involved in the regulation of a functionally important transcriptional module shared by both T_{reg} and T_H2 effector T cells. To test this hypothesis, we cross-referenced the IRF4-dependent gene data set derived from our T_{reg} cell studies to an effector T_H2-specific gene data set. This comparison and independent qPCR analysis showed that in addition to *Icos*, the expression of two important T_H2 genes *Maf* and *Ccr8* was compromised in IRF4-deficient T_{reg} cells, and the expression *Il1rl* — another essential player in T_H2 differentiation —was also decreased (Fig. 5f–h)[27–29].

Next, using *Icos* as a model gene, we sought to investigate the possibility that in T_{reg} cells IRF4 and Foxp3 co-operate in transcriptional regulation. Using CLOVER, a transcription factor binding site prediction algorithm[30], we identified a putative IRF4 binding site within the *Icos* promoter corresponding to the Foxp3 binding sites[4] (Supplementary Fig. 8), and confirmed binding of both Foxp3 and IRF4 by ChIP-coupled qPCR (Fig. 5i). These results raised the possibility that Foxp3 physically interacts with IRF4. In fact, this interaction was confirmed by IRF4 and Foxp3 co-immunoprecipitation from T_{reg} cell nuclear lysates using a Foxp3-specific antibody (Fig. 5j). These results indicate that IRF4 binds to Foxp3 and the resulting complexes affect expression of certain target genes such as *Icos*.

Our results indicate that Foxp3 induces IRF4 expression in T_{reg} cells. A transcriptional module downstream of IRF4 is probably modified after IRF4 interaction with Foxp3 to facilitate efficient T_H2 suppression by T_{reg} cells. Uniformly increased IRF4 protein expression in peripheral T_{reg} cells seems to suggest that they are equally poised to suppress T_H2 responses. However, T_{reg} cell populations may still be heterogeneous in this regard, if signalling-dependent post-translational modifications of IRF4 or recruitment of other nuclear factors are needed for T_{reg}-mediated T_H2 suppression. We propose that T_{reg} cells might hijack certain components of transcriptional machinery promoting a particular effector T cell differentiation to efficiently control the corresponding type of the immune response.

Methods Summary

Mice

Mice containing $Irf4^{fl}$, $Irf4^{-}$, $Foxp3^{Cre}$ and $Foxp3^{DTR}$ alleles were previously described[7,18,19]. The $Irf4^{fl/fl}Foxp3^{Cre}$ and $Irf4^{fl/-}$ $Foxp3^{Cre}$ mice were indistinguishable in regards to the IRF4 deletion efficiency in T_{reg} cells and to the immunological and clinical manifestations of

autoimmunity, and so were all three types of healthy littermate control mice, *Irf4*$^{+/+}$ *Foxp3*^{Cre}, *Irf4*$^{fl/+}$ *Foxp3*^{Cre} and *Irf4*$^{+/-}$ *Foxp3*^{Cre}.

Flow cytometric and serum immunoglobulin analyses

Rat anti-mouse IRF4 monoclonal antibody (clone 3E4) was raised against a glutathione *S*-transferase (GST)-fusion protein containing the carboxy-terminal 65-amino-acid sequence of murine IRF4. FACS data were acquired on a FACSCanto flow cytometer (Becton Dickinson) and analysed using FlowJo software package (Tri-Star).

Serum IgM, IgG1, IgG2a, IgG2b, IgG3 and IgA concentrations were measured using SBA Clonotyping System (Southern Biotech). IgE ELISA was performed using biotinylated anti-IgE antibody (BD Pharmingen) and streptavidin-conjugated HRP.

ChIP and qPCR

ChIP with Foxp3 and IRF4 antibodies (Santa Cruz Biotechnology) were performed using MACS-purified CD4$^+$ CD25$^+$ T_{reg} cells as previously described[4]. qPCRs were performed using primers listed in Supplementary Table 1.

Methods

Mice

C57BL/6 (B6) mice were purchased from the Jackson Laboratory. Mice containing *Irf4*^{fl}, *Irf4*$^{-}$, *Foxp3*^{Cre} and *Foxp3*^{DTR} alleles were previously described[7,18,19]. The *Irf4*$^{fl/fl}$*Foxp3*^{Cre} mice were indistinguishable from *Irf4*$^{fl/-}$ *Foxp3*^{Cre} mice in regards to the efficiency of IRF4 deletion in T_{reg} cells, and to the immunological and clinical manifestations of autoimmunity, as were all three types of healthy littermate control mice, *Irf4*$^{+/+}$ *Foxp3*^{Cre}, *Irf4*$^{fl/+}$ *Foxp3*^{Cre} and *Irf4*$^{+/-}$ *Foxp3*^{Cre}. Mice were housed under specific pathogen-free conditions and used according to the guidelines of the Institutional Animal Care Committee at the University of Washington.

Antibodies and FACS analysis

Fluorescent-dye-conjugated antibodies were purchased from BD Pharmingen and eBioscience. Rat anti-mouse IRF4 monoclonal antibody (clone 3E4) was raised against a GST-fusion protein containing the C-terminal 65-amino-acid sequence of murine IRF4. FACS data were acquired on a FACSCanto flow cytometer (Becton Dickinson) and analysed using FlowJo software package (Tri-Star). Intracellular staining of Foxp3 and IRF4 was conducted using Foxp3 Mouse Regulatory T cell Staining Kit (eBioscience). For flow cytometric analysis of cytokine- and immunoglobulin-secreting cells, cell populations were first stained with antibodies against the indicated cell surface markers, followed by permeabilization in Fix/Perm buffer, and intracellular staining in Perm/Wash buffer (BD Pharmingen).

Immunofluorescence microscopy

Frozen tissue sections were fixed in cold acetone for 20 min, washed twice and pre-blocked in PBS containing 5% normal rat serum, 5% normal rabbit serum and 5% BSA for 30 min. Slides were then incubated in primary antibodies (anti-GL7-FITC, anti-IgD-biotin, anti-CD4-AF647) for 45 min, washed twice, and incubated with secondary antibodies (anti-FITC-AF488, StrepAv-AF555) for 45 min and fluorescence was examined using a Leica SL confocal microscope.

In vitro suppression assay

For *in vitro* suppression assays, T_{reg} cells and 'effector' T cells were purified by positive selection using CD4-specific MACS beads (Miltenyi), followed by sorting on a FACSAria cell sorter (Becton Dickinson). Antigen-presenting cells were prepared from wild-type B6 splenocytes by T-cell depletion using Thy1-specific MACS beads. Effector T cells (2×10^4 cells well^{-1}) were co-cultured with T_{reg} cells at indicated ratios in the presence of irradiated (30 Gy) antigen-presenting cells (1×10^5 cells well^{-1}) in 96-well plates in complete RPMI1640 medium supplemented with 10% FBS and CD3 antibody (1 μg ml^{-1}) for 60 h. One microcurie ^{3}H-thymidine was added into the cultures for a further 8–12 h and cell proliferation in triplicate cultures was measured using a scintillation counter.

Serum immunoglobulin ELISA

Serum IgM, IgG1, IgG2a, IgG2b, IgG3 and IgA concentrations were measured using SBA Clonotyping System (Southern Biotech). For IgE, ELISA was performed using biotinylated anti-IgE detection antibody (BD Pharmingen) and streptavidin-conjugated HRP.

Affymetrix microarray and qRT–PCR

Total RNA was extracted with RNA Stat-60 reagent (Iso-Tex Diagnostics) from IRF4-sufficient and -deficient CD4$^+$ GFP/YFP-Cre$^+$ T_{reg} cells FACS-purified from healthy *Irf4*$^{+/-}$ *Foxp3*^{Cre} and *Irf4*$^{fl/-}$ *Foxp3*$^{Cre/wt}$ mice, respectively. Complementary DNA was synthesized using Superscript II Reverse Transcriptase (Invitrogen), and amplified twice and labelled using MessageAmp II aRNA Amplification kit (Ambion). Biotinylated complementary RNA was fragmented and hybridized to Affymetrix GeneChip Mouse Genome 430 2.0 arrays at the Stanford PAN Facility. All data analyses were performed by using Bioconductor for the statistical software R (http://www.r-project.org). Expression values were background corrected, normalized and summarized by using the default settings of the gcrma package. From the resulting data sets we extracted a list of genes with a more than twofold change in expression and cross-referenced this list to the previously published set of T_{reg}-specific genes[9]. Effector T_H2-specific gene data set was extracted by subtracting gene expression values for CD4 T cells activated *in vitro* under T_H1 skewing conditions or without skewing (T_H0) from those for T cells activated under T_H2 skewing conditions (K. Hilgner and K. Murphy, unpublished observations).

To verify expression array data, independently prepared T_{reg} cell samples were used to generate cDNA. qPCR was performed using Power SYBR Green PCR master mix (Applied Biosystems). PCR primer sequences are listed in Supplementary Table 1.

Chromatin immunoprecipitation and qPCR

Foxp3 and IRF4 antibody (Santa Cruz Biotechnology) ChIPs were performed using MACS purified CD4$^+$ CD25$^+$ T_{reg} cells as previously described[4]. qPCRs were performed using primers listed in Supplementary Table 1.

Immunoprecipitation and western blot analysis

Nuclear extracts from sorted CD4$^+$ Foxp3$^+$ and CD4$^+$ Foxp3$^-$ cells were prepared in nuclear lysis buffer (Active Motif) according to the manufacturer's protocol. Immunoprecipitation was carried out using anti-Foxp3-coated magnetic beads followed by western blotting with Foxp3, IRF4 or p65 antibodies.

Supplementary Material

Refer to Web version on PubMed Central for supplementary material.

Acknowledgments

We thank K. Hilgner and K. Murphy for providing T_H1, T_H2 and T_H0 gene expression data sets, B. Sullivan, R. Locksley, S. Quezada and J. Allison for critical reagents, K. Forbush and L. Karpik for expert technical assistance and mouse colony management, and R. Dalla-Favera for discussions. This work was supported by grants from the National Institutes of Health (A.Y.R.). Y.Z.and J.M.K. were supported by the CRI-Irvington Institute postdoctoral fellowship. A.Y.R. is an investigator with the Howard Hughes Medical Institute.

References

1. Ramsdell F. Foxp3 and natural regulatory T cells: key to a cell lineage? Immunity 2003;19:165–168. [PubMed: 12932350]
2. Sakaguchi S, et al. Foxp3$^+$ CD25$^+$ CD4$^+$ natural regulatory T cells in dominant self-tolerance and autoimmune disease. Immunol Rev 2006;212:8–27. [PubMed: 16903903]
3. Zheng Y, Rudensky AY. Foxp3 in control of the regulatory T cell lineage. Nature Immunol 2007;8:457–462. [PubMed: 17440451]
4. Zheng Y, et al. Genome-wide analysis of Foxp3 target genes in developing and mature regulatory T cells. Nature 2007;445:936–940. [PubMed: 17237761]
5. Marson A, et al. Foxp3 occupancy and regulation of key target genes during T-cell stimulation. Nature 2007;445:931–935. [PubMed: 17237765]
6. Kanangat S, et al. Disease in the scurfy (sf) mouse is associated with overexpression of cytokine genes. Eur J Immunol 1996;26:161–165. [PubMed: 8566060]
7. Kim JM, Rasmussen JP, Rudensky AY. Regulatory T cells prevent catastrophic autoimmunity throughout the lifespan of mice. Nature Immunol 2007;8:191–197. [PubMed: 17136045]
8. Fontenot JD, et al. Regulatory T cell lineage specification by the forkhead transcription factor foxp3. Immunity 2005;22:329–341. [PubMed: 15780990]
9. Gavin MA, et al. Foxp3-dependent programme of regulatory T-cell differentiation. Nature 2007;445:771–775. [PubMed: 17220874]
10. Lin W, et al. Regulatory T cell development in the absence of functional Foxp3. Nature Immunol 2007;8:359–368. [PubMed: 17273171]
11. Williams LM, Rudensky AY. Maintenance of the Foxp3-dependent developmental program in mature regulatory T cells requires continued expression of Foxp3. Nature Immunol 2007;8:277–284. [PubMed: 17220892]
12. Eisenbeis CF, Singh H, Storb U. Pip, a novel IRF family member, is a lymphoid-specific, PU.1-dependent transcriptional activator. Genes Dev 1995;9:1377–1387. [PubMed: 7797077]
13. Mittrucker HW, et al. Requirement for the transcription factor LSIRF/IRF4 for mature B and T lymphocyte function. Science 1997;275:540–543. [PubMed: 8999800]
14. Iida S, et al. Deregulation of MUM1/IRF4 by chromosomal translocation in multiple myeloma. Nature Genet 1997;17:226–230. [PubMed: 9326949]
15. Lohoff M, et al. Dysregulated T helper cell differentiation in the absence of interferon regulatory factor 4. Proc Natl Acad Sci USA 2002;99:11808–11812. [PubMed: 12189207]
16. Rengarajan J, et al. Interferon regulatory factor 4 (IRF4) interacts with NFATc2 to modulate interleukin 4 gene expression. J Exp Med 2002;195:1003–1012. [PubMed: 11956291]
17. Brustle A, et al. The development of inflammatory T_H-17 cells requires interferon-regulatory factor 4. Nature Immunol 2007;8:958–966. [PubMed: 17676043]
18. Klein U, et al. Transcription factor IRF4 controls plasma cell differentiation and class-switch recombination. Nature Immunol 2006;7:773–782. [PubMed: 16767092]
19. Rubtsov YP, et al. Regulatory T cell-derived interleukin-10 limits inflammation at environmental interfaces. Immunity 2008;28:546–558. [PubMed: 18387831]
20. Collison LW, et al. The inhibitory cytokine IL-35 contributes to regulatory T-cell function. Nature 2007;450:566–569. [PubMed: 18033300]
21. Li MO, Wan YY, Flavell RA. T cell-produced transforming growth factor-β1 controls T cell tolerance and regulates Th1- and Th17-cell differentiation. Immunity 2007;26:579–591. [PubMed: 17481928]

22. Takahashi T, et al. Immunologic self-tolerance maintained by $CD25^+$ $CD4^+$ regulatory T cells constitutively expressing cytotoxic T lymphocyte-associated antigen 4. J Exp Med 2000;192:303–310. [PubMed: 10899917]

23. Kobie JJ, et al. T regulatory and primed uncommitted CD4 T cells express CD73, which suppresses effector CD4 T cells by converting 5′-adenosine monophosphate to adenosine. J Immunol 2006;177:6780–6786. [PubMed: 17082591]

24. Deaglio S, et al. Adenosine generation catalyzed by CD39 and CD73 expressed on regulatory T cells mediates immune suppression. J Exp Med 2007;204:1257–1265. [PubMed: 17502665]

25. Cao X, et al. Granzyme B and perforin are important for regulatory T cell-mediated suppression of tumor clearance. Immunity 2007;27:635–646. [PubMed: 17919943]

26. Nurieva RI, et al. Transcriptional regulation of Th2 differentiation by inducible costimulator. Immunity 2003;18:801–811. [PubMed: 12818161]

27. Ho IC, Lo D, Glimcher LH. c-maf promotes T helper cell type 2 (Th2) and attenuates Th1 differentiation by both interleukin 4-dependent and -independent mechanisms. J Exp Med 1998;188:1859–1866. [PubMed: 9815263]

28. Chensue SW, et al. Aberrant *in vivo* T helper type 2 cell response and impaired eosinophil recruitment in CC chemokine receptor 8 knockout mice. J Exp Med 2001;193:573–584. [PubMed: 11238588]

29. Lohning M, et al. T1/ST2 is preferentially expressed on murine Th2 cells, independent of interleukin 4, interleukin 5, and interleukin 10, and important for Th2 effector function. Proc Natl Acad Sci USA 1998;95:6930–6935. [PubMed: 9618516]

30. Frith MC, et al. Detection of functional DNA motifs via statistical over-representation. Nucleic Acids Res 2004;32:1372–1381. [PubMed: 14988425]

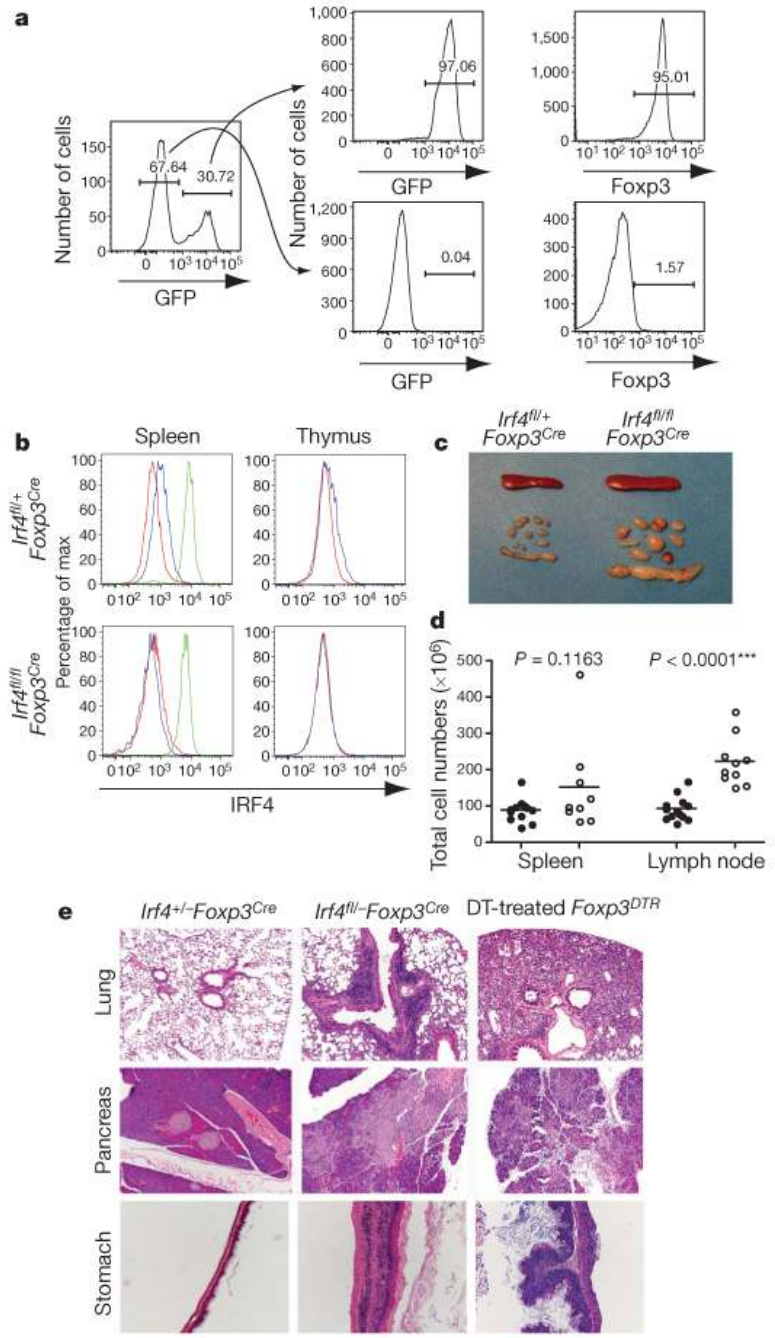

Figure 1. Ablation of IRF4 in T_{reg} cells results in autoimmune lymphoproliferative disease

a, *Foxp3*^{Cre}-mediated deletion of *Irf4* is restricted to T_{reg} cells. Spleen and lymph node CD4$^+$ T cells from *Irf4*$^{fl/-}$ *Foxp3*^{Cre} mice were FACS-sorted into GFP$^+$ and GFP$^-$ cells containing a recombined and unrecombined *Irf4*^{fl} allele, respectively, and stained for Foxp3. The post-sorting purity of GFP$^+$ and GFP$^-$ population was greater than 97%. **b**, Intracellular staining of IRF4 in splenic and thymic CD4$^+$ Foxp3$^-$ (red) and CD4$^+$ Foxp3$^+$ (blue) cells and splenic B220$^-$ CD138$^+$ (green) plasma cells (positive control) in *Irf4*$^{fl/+}$ *Foxp3*^{Cre} (top panels) and *Irf4*$^{fl/fl}$*Foxp3*^{Cre} mice (bottom panels). **c**, Splenomegaly and lymphadenopathy in *Irf4*$^{fl/fl}$*Foxp3*^{Cre} mice. **d**, Spleen and lymph node cellularity in *Irf4*$^{fl/+}$ *Foxp3*^{Cre} (filled circles) and *Irf4*$^{fl/fl}$*Foxp3*^{Cre} (open circles) mice. **e**, Histopathology induced after IRF4 ablation in

T_{reg} cells. Representative haematoxylin and eosin (H&E)-stained tissue sections from 8-week-old *Irf4*$^{+/-}$ *Foxp3*^{Cre} and *Irf4*$^{fl/-}$*Foxp3*^{Cre} mice and diphtheria-toxin-treated *Foxp3*^{DTR} mice. Note pronounced infiltrates in the lung, pancreas and stomach of *Irf4*$^{fl/-}$ *Foxp3*^{Cre} mice and severe lesions in tissues from diphtheria-toxin-treated *Foxp3*^{DTR} mice (n = 3–5). Original magnification (**c**, **e**), ×10.

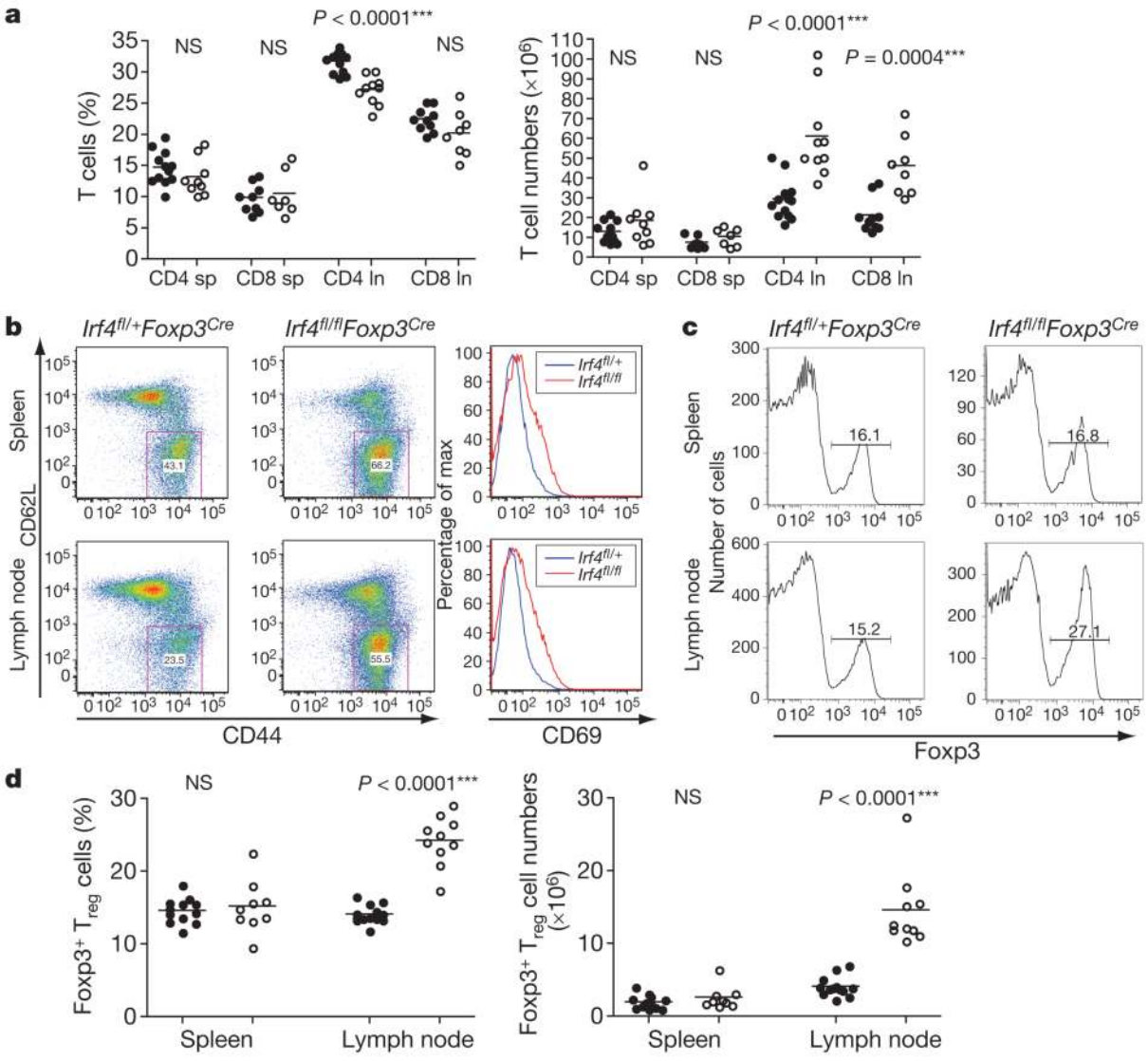

Figure 2. Increased numbers and activation of CD4$^+$ T cells in mice harbouring IRF4-deficient T$_{reg}$cells

a, CD4$^+$ and CD8$^+$ T cell numbers in the spleen (sp) and lymph nodes (ln) of *Irf4$^{fl/fl}$Foxp3^{Cre}* (open circles) mice and *Irf4$^{fl/+}$ Foxp3^{Cre}* (filled circles) littermate control mice. NS, not significant. **b**, Flow cytometric analysis of CD44, CD62L and CD69 expression on CD4$^+$ T cells in 8-week-old *Irf4$^{fl/fl}$Foxp3^{Cre}* mice and *Irf4$^{fl/+}$ Foxp3^{Cre}* littermates. A representative of three independent experiments is shown. **c, d,** Increased Foxp3$^+$ T$_{reg}$ cell subset in *Irf4$^{fl/fl}$Foxp3^{Cre}* mice. Flow cytometric analyses of spleen and lymph node cells from *Irf4$^{fl/+}$ Foxp3^{Cre}* (filled circles) and *Irf4$^{fl/fl}$Foxp3^{Cre}* (open circles) mice. A representative of three independent experiments is shown.

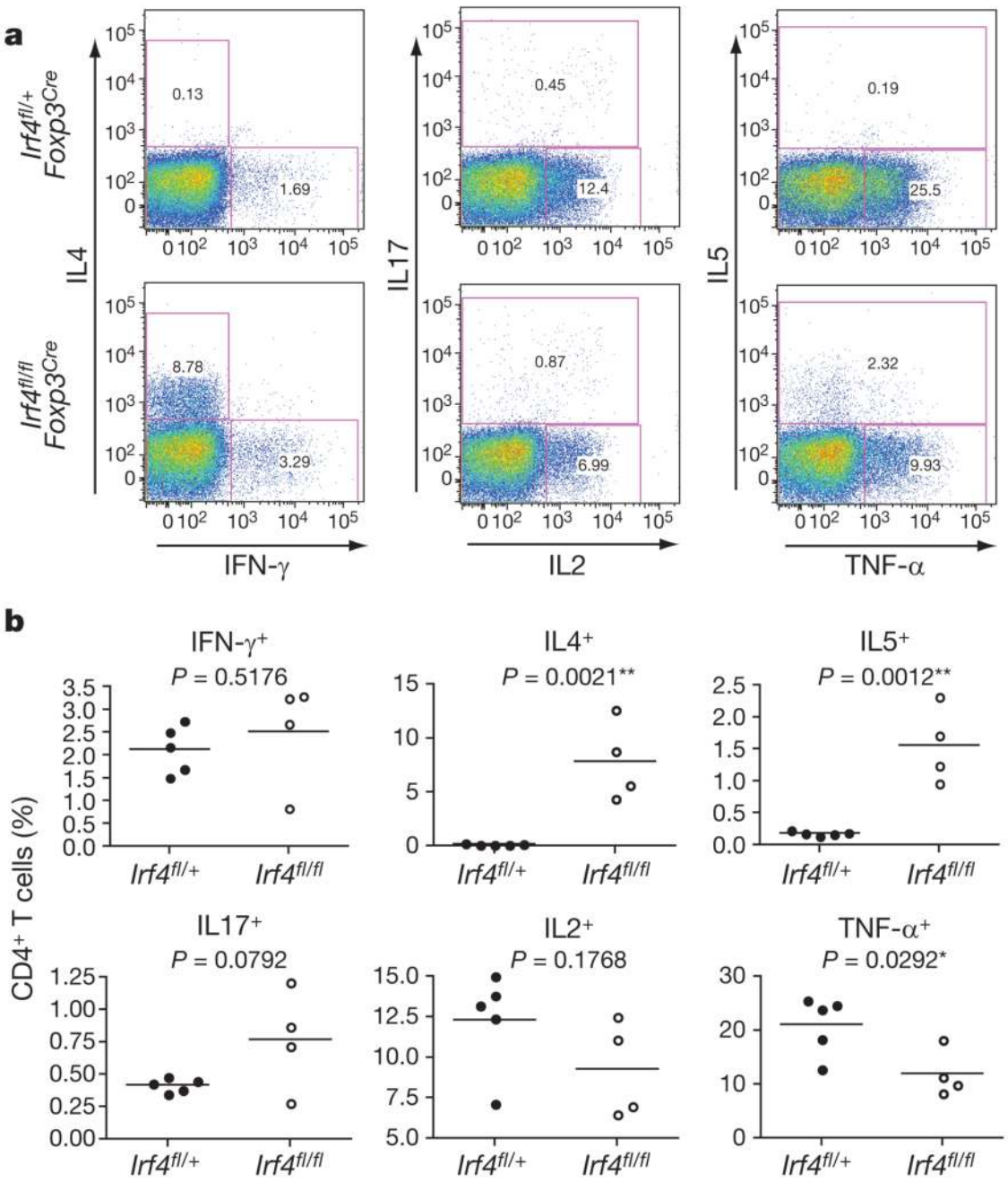

Figure 3. IRF4 deficiency in T_{reg} cells results in a selective failure to control T_H2 responses

a, b, Flow cytometric analysis of cytokine production by splenic $CD4^+$ T cells from *Irf4*$^{fl/+}$ *Foxp3*^{Cre} mice and *Irf4*$^{fl/fl}$*Foxp3*^{Cre} littermates. Splenocytes were stimulated with CD3 (5 μg ml^{-1}) and CD28 (5 μg ml^{-1}) antibodies in the presence of Golgi-Plug (1 μg ml^{-1}) for 5 h before staining for CD4, CD8 and the indicated cytokines. A representative of three independent experiments is shown.

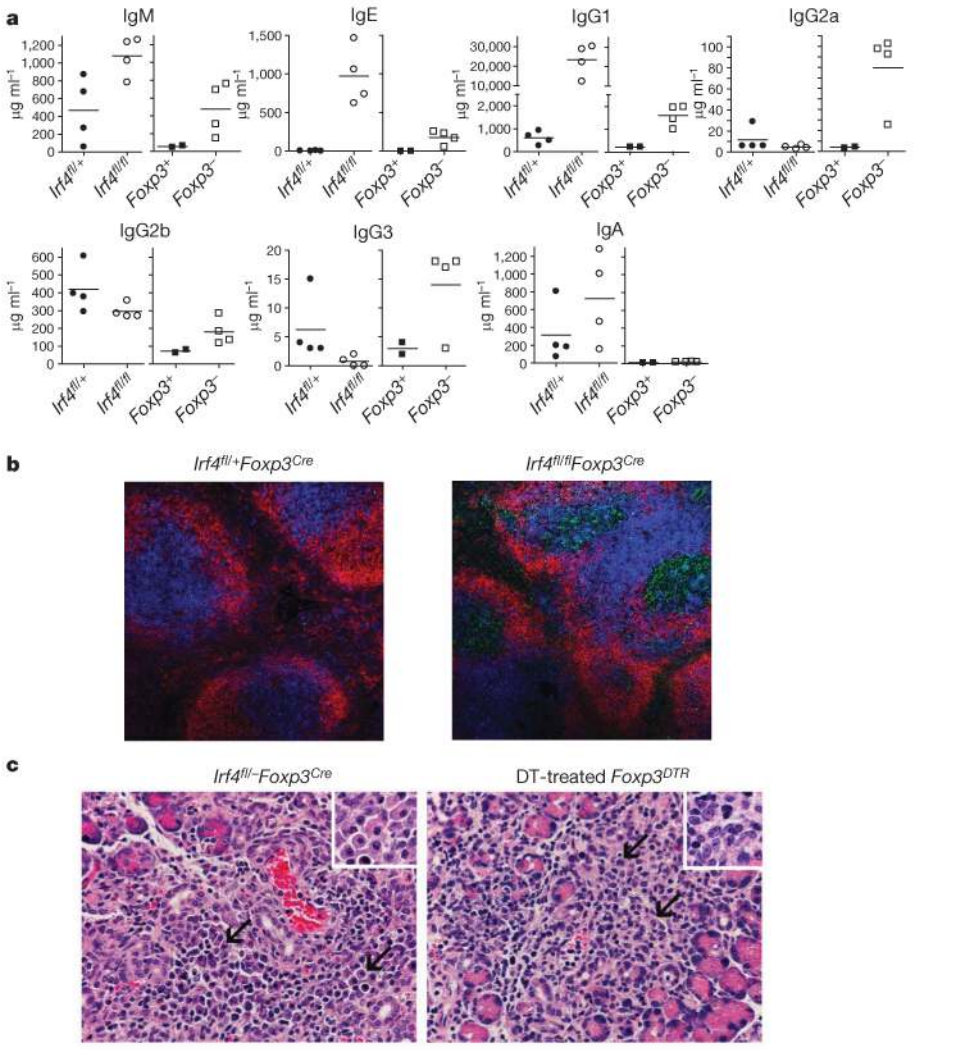

Figure 4. Increased serum IgG1 and IgE concentration, germinal centre formation, and plasma cell tissue infiltration caused by IRF4 deficiency in T_{reg} cells

a, Analysis of immunoglobulin isotype amounts in sera of 8-week-old *Irf4*$^{fl/fl}$*Foxp3*^{Cre} mice and *Irf4*$^{fl/+}$ *Foxp3*^{Cre} littermates, and of 3–4-week-old *Foxp3*$^{-}$ and *Foxp3*$^{+}$ littermates. **b**, Immunofluorescent staining of germinal centre B cells (GL7^{+}, green), follicular B cells (IgD^{+}, red), and CD4^{+} T cells (blue) in spleens of *Irf4*$^{fl/fl}$*Foxp3*^{Cre} mice and *Irf4*$^{fl/+}$ *Foxp3*^{Cre} littermates. Original magnification, ×20. **c**, Histological sections of H&E-stained pancreas from 8-week-old *Irf4*$^{fl-}$ *Foxp3*^{Cre} mice and T_{reg}-deficient diphtheria-toxin-treated *Foxp3*^{DTR} mice. The *Irf4*$^{fl/-}$ *Foxp3*^{Cre} pancreas is infiltrated primarily by plasma cells (arrows), that is, distinct round cells containing an eccentric nucleus with a cartwheel chromatin appearance and perinuclear clearing (inset; original magnification, ×60). In contrast, the pancreatic infiltrates of diphtheria-toxin-treated *Foxp3*^{DTR} mice contained principally macrophages (arrows), that is, large cells with abundant eosinophilic cytoplasm, reniform to oval nuclei, and indistinct cell borders (inset; original magnification, ×60). Original magnification for both panels, ×40. Representative sections are shown.

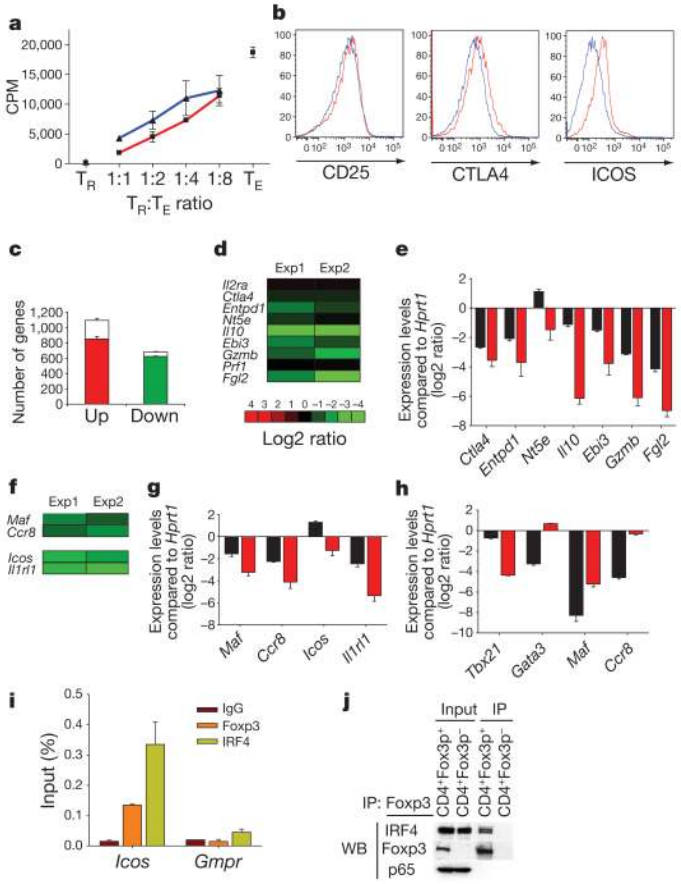

Figure 5. IRF4 interacts with Foxp3 and diminished expression of a subset of suppressor effector and T_H2 specific genes in IRF4-deficient T_{reg} cells

a, IRF4-sufficient (*Irf4*$^+$ T_R, red) and -deficient (*Irf4*$^-$ T_R, blue) T_{reg} cells from 5-week-old *Irf4*$^{+/+}$ *Foxp3*^{Cre} mice and *Irf4*$^{fl/fl}$*Foxp3*^{Cre} littermates suppress *in vitro* proliferative response of Foxp3$^-$ CD4$^+$ T cells (T_E) from B6 mice. A representative of two independent experiments is shown. **b**, Flow cytometric analysis of CD25, CTLA4 and ICOS expression by IRF4-sufficent (red) and -deficient (blue) T_{reg} cells. **c**, Numbers of IRF4-independent genes that were up- (red bars) or downregulated (green bars), respectively, in T_{reg} cells compared to naive CD25$^-$ Foxp3$^-$ CD4$^+$ T cells[9]. Open bars represent genes in which expression was changed by twofold or more in the absence of IRF4. **d**, Decreased expression of genes with a presumed role in T_{reg} suppressor function in IRF4-deficient compared to IRF4-sufficient T_{reg} cells. The data (**c, d**) represent average of two independent microarray experiments (exp) performed using YFP-Cre$^+$ T_{reg} cells FACS-purified from healthy *Irf4*$^{fl/-}$ *Foxp3*$^{Cre/wt}$ and *Irf4*$^{+/-}$ *Foxp3*^{Cre} littermates. **e**, qPCR analysis of relative expression of genes shown in **d** in *Irf4*$^+$ T_{reg} (black) and *Irf4*$^-$ T_{reg} (red). **f**, The decreased expression of T_H2-specific or functionally important genes in IRF4-deficient in comparison to IRF4-sufficient T_{reg} cells (two independent microarray experiments as above). **g**, **h**, qPCR analysis of relative expression of the T_H2-specific gene set in *Irf4*$^+$ T_{reg} (black) and *Irf4*$^-$ T_{reg} (red) (**g**), and in *in vitro* differentiated T_H1 (black) and T_H2 cells (red) (**h**). Data in **e, g** and **h** represent mean and s.d. of the expression of genes relative to *Hprt1* in two independent experiments using three replicates each. i, Both IRF4 and Foxp3 bind to the promoter region of the *Icos* gene. qPCR analysis of Foxp3- and IRF4-bound chromatin isolated from wild-type T_{reg} cells using primer set corresponding to the *Icos* promoter region. IgG ChIP and qPCR using primers corresponding to the promoter region of *Gmpr* was used as a specificity controls. **j**, Western blot (WB) analysis of IRF4 in

nuclear lysates of wild-type Foxp3$^+$ T_{reg} cells and total Foxp3$^-$ CD4$^+$ T cells (control) (lanes 1 and 2), and in Foxp3 complexes immunoprecipitated (IP) from the nuclear lysates using Foxp3 antibody. Transcription factor p65 was a negative control. IRF4 signal in control nuclear lysates is due to the presence of activated IRF4$^+$ CD25$^+$ Foxp3$^-$ T cells.